



## The Influence of the Inclusion of Nano Ceramic Particles on the PMMA Composite Properties for Biomaterials Applications



Aya A. Shaher\*, Assel B. Al.Zubaidi, Wafaa M. Salih

Materials Engineering Dept., University of Technology-Iraq, Alsina'a street, 10066 Baghdad, Iraq.

\*Corresponding author Email: [ayashahir3@gmail.com](mailto:ayashahir3@gmail.com)

### HIGHLIGHTS

- Applying ceramic nanoparticles as reinforcement to PMMA soft acrylic resin.
- Using the ultrasonic mixing method to dispersion nanoparticles into the matrix.
- Study the mechanical and physical characteristics of the nanocomposite samples.
- Identifying the biological activity of PMMA/Nano-ceramic powder by determining the antibacterial activity.

### ARTICLE INFO

**Handling editor:** Omar H. Hassoon

**Keywords:**

PMMA  
TiO<sub>2</sub>  
SiO<sub>2</sub>  
Talc  
Bio nanocomposites  
Nanoparticles  
Mechanical properties  
Physical properties

### ABSTRACT

This study examines the effects of reinforcing PMMA acrylic resin with different Nanoparticle types: Silica (SiO<sub>2</sub>) (67.8nm), Titania (TiO<sub>2</sub>) (57.3nm), and Talc powders (TP) (80.1nm). This was done by using the ultrasonic mixing method for dispersing the nano-powder in the matrix and using them at three different proportions (0.5, 1, and 1.5%) to improve the properties of PMMA composite materials for medical applications. The characteristic functional groups associated with Nano-ceramic particles and PMMA in the composite specimens were confirmed by FT-IR spectroscopy. Also, this research investigates some mechanical properties, including (tensile strength, compression strength, elastic modulus, hardness, and surface roughness), some physical properties (density and water absorption), and biological properties (antibacterial activity). The experimental work was performed on prepared specimens that may be employed for cartilaginous joint applications. The results revealed that all mechanical properties enhanced as the nanoparticles concentration was increased till it reached a maximum of 1.5%. The proportion of tensile strength and elastic modulus enhancement for 1.5% of (SiO<sub>2</sub>, TiO<sub>2</sub>, and Talc) is equal to (66.5%, 47.55% and 59.38%), (261.5, 315.38 and 388.4%), respectively. The compressive strength of composites increased by (49.3, 36.66, and 40.5%) for 1.5% (SiO<sub>2</sub>, TiO<sub>2</sub>, and Talc). The physical properties manifested that the increased content of reinforcing nanoparticles led to the raised water absorption, while the density values of PMMA nanocomposite decreased. Additionally, the biological results elucidated that the increased concentration led to the increased antibacterial activity of nanocomposite. Furthermore, the results concluded that adding 1.5% of SiO<sub>2</sub> to a PMMA matrix improves the properties obtained.

## 1. Introduction

Biomaterial areas have been a captivating subject of study for many researchers from several disciplines [1]. A biomaterial is a material that is permanently or intermittently in communication with bodily fluids and is meant to interact with biological systems to assess, repair, enhance, or replace the human body function, tissue, or organ [2]. Acrylic, also known as polymethylmethacrylate (PMMA), has been employed in biological applications since the early 1900s. Initially, PMMA was utilized for hard contact lenses which was accidentally found because of its biocompatible nature. PMMA is additionally utilized in dentistry applications as an essential material in the production of dentures. Then, the "dental acrylic" is then used in arthroplasty surgery of the total hip to cement an orthopedic prosthesis [2,3]. PMMA is a linear thermoplastic polymer with long backbone carbon chains that are smoother and thinner, allowing them to slide more readily together, and making the material softer [4]. It has several advantages, including ease of processability, lightweight, low fabrication cost, lack of toxicity, and high biostability in the human body. But, due to the inadequate biological and mechanical properties of PMMA, preliminary clinical outcomes were unsatisfactory. For instance, lack of antibacterial, poor level of bioactivity (bioinert material), and mechanical performance is considered the drawbacks of PMMA, which limit its clinical applications [3,5]. Many studies focused on enhancing the mechanical or biological properties of PMMA, primarily by including additives as reinforcement materials. Owing

to the unique properties of materials in the nanoscale that cannot be achieved without nano [6], many researchers in various medical domains have turned to nanomaterials for their physicochemical qualities, such as highly tiny shape, extremely high surface area to mass ratios, and improved chemical reactivity. Nanomaterials are minimal and have a variety of advanced physical and chemical features. Because of their small size, nanoparticles can easily enter microbial cells and induce inhibitory processes. Nanoparticles have been employed as antibacterial agents since they can be bacteriostatic or bactericidal by reducing their food source or damaging their cell membrane [7]. This research uses ultrasonic mixing to reinforce the PMMA polymer matrix with nano-ceramic particles ( $\text{TiO}_2$ ,  $\text{SiO}_2$ , and Talc). The literature review comprises some studies that have been completed on this topic.

Lie et al. estimated the influence of different weight ratios of Akermanite ( $\text{Ca}_2\text{MgSi}_2\text{O}_7$ , AKT) powders on the characteristics of (PMMA) matrix trying to fix the defects of PMMA having low mechanical and osseointegration and high exothermic reactions. The result of mechanical tests showed that with the increase in loading of AKT powders into the PMMA matrix, there was no significant difference in compressive strength of (4.8%) at 50wt.% of AKT powder and a slight increase in elastic modulus of (20%) at 50wt.% of AKT powder. Additionally, this addition improved its osteogenic activity, with a substantially reduced temperature of polymerization obtained from the filler content variety compared with the pure PMMA [8].

Pahlevanzadeh et al. studied the influence of Monticellite (Mon) and carbon nanotubes (CNTs) at different weight ratios on the mechanical properties and bioactivity of PMMA in order to treat the issue of bone defects. This examination revealed that an additional 0.5 weight ratio of (CNTs) into the PMMA-Mon cement has a significant increase in elastic modulus (56.25%), ultimate tensile strength (29.3%), and elongation (62%), with ideal bioactivity results than PMMA-Mon cement and pure PMMA tested [9].

Bdaiwi examined the effect of adding nano zirconium titanium yttrium ( $\text{ZrO}_2\text{Y}_2\text{O}_3$ ) particles with weight percentages (0.5, 1, 1.5, 2, and 2.5%) on the mechanical properties of PMMA to cure the problem of PMMA fragility. The result depicted that adding 1% of ( $\text{ZrO}_2\text{Y}_2\text{O}_3$ ) nanoparticles to the basic material (PMMA) led to improved flexural strength at (20%), Young's modulus (8.2%), elongation at break (78.5%), impact strength (46.15%), fracture toughness (42.8%), compression strength (15.38%) and bending modulus (23.33%), while the hardness value decreased with adding nanoparticles [10].

Obeid et al. investigated the PMMA mechanical properties reinforced with zirconium dioxide Nano-crystal ( $\text{ZrO}_2$ ) with weight ratios (1, 2, 3, 4, and 5%) used in medical applications as compensatory materials to teeth and bones. The result indicated that incorporating 5% $\text{ZrO}_2$  nanoparticle into the matrix produced a nanocomposite sample with a significant improvement in the surface hardness value (157.14%), impact strength value (226.66%), Young's modulus value (370%), and value of compression resistance (116.5%) with increasing the ratios for reinforcing material compared with the pure PMMA [11].

Anamarija et al. studied the influence of adding ( $\text{TiO}_2$ ) nanoparticles to polymethylmethacrylate (PMMA) to use as restorations with low toxicity and high mechanical performance. The study's findings illustrated the reduced mechanical performance of PMMA composite specimens by increasing the quantity of  $\text{TiO}_2$ . At the same time, the antibacterial results evinced that the addition of  $\text{TiO}_2$  nanoparticles significantly affected the formation of *S. mutans* biofilm on the PMMA composite sample surface. Adding (10%) and (20%) of  $\text{TiO}_2$  resulted in a single bacterial adhesion decay that is equal to (58%) and (60%), respectively [12].

Shirazia et al. estimated the consequence of incorporating ( $\text{Al}_2\text{O}_3$ ) and (HA) nanoparticles with varying volume divisions on the mechanical and tribological characteristics of PMMA composite materials. The results appeared that combining (3wt.%) alumina ( $\text{Al}_2\text{O}_3$ ) nanoparticles with the PMMA cement matrix achieved a significant enhancement of the hardness (25%) and the elastic modulus (90%) values compared to the other PMMA/ $\text{Al}_2\text{O}_3$  nanocomposites. Additionally, the nanocomposite bone cement containing (5 wt.%) of  $\text{Al}_2\text{O}_3$  and (5 wt.%) of HA exhibited better properties compared to the other PMMA/HA/ $\text{Al}_2\text{O}_3$  nanocomposites [13].

Abdullah et al. demonstrated the influence of incorporating (1, 2, 3, 4, and 5wt.%) of treated and untreated eggshell powder (ESP) into PMMA polymer matrix on the composite's strength of impact, the modulus of flexural and the rate of wear. The results manifested that the increased eggshell contents improved the mechanical properties of the PMMA/ESP composites. Additionally, since the interface bond between the polymer and the particles has strengthened, the calcination procedure of eggshell powder particles enhanced the PMMA composite specimen's characteristics compared to the untreated eggshell powder at a similar weight proportion. The best improvement of impact test (100%) and modulus of flexural (28%) with a decrease in wear rate (60%) was achieved by adding 3wt.% of treated ESP [14].

Choudhary et al. conducted a study of the effect of adding (diopside;  $\text{CaO-MgO-2SiO}_2$ ) as a bioactive ceramic reinforcement filler to PMMA to provide adequate osteoconductivity (bioactive) and mechanical stability to be utilized for repairing the bone defects. The results demonstrated that the prepared composites reinforced with (50%) diopside had acceptable mechanical properties and good apatite deposition ability; compressive strength (400%), Young's modulus (300%), and generated apatite deposition on the surface after immersion for four weeks in the SBF solution [4].

Al-Janabi et al. investigated the effects of adding various ratios (0.5, 1, 1.5, and 2 wt.%) of treated  $\text{TiO}_2$  nanoparticles with a silane coupling agent to a polymethylmethacrylate (PMMA) matrix on the mechanical properties to solve the PMMA weakness mechanical resistance. The results elucidated that the maximum values of mechanical properties achieved by incorporating (1wt.%) of modified  $\text{TiO}_2$  nano-powder led to an increase of (93%) in bending strength, and the compression strength improved by (39.31%) and subsequently declined to the point where the (1 wt.%) refers to the optimal percentage; the morphological conclusions confirmed the mechanical performances [15].

Bashir, et al. prepared nanocomposites of PMMA polymer reinforced with weight ratios (0, 1, 2, 3, and 4%) from Bio-glass ceramic nano-powder and studied the hardness and fatigue of the nanocomposite prepared. The results portrayed that when the weight ratios of a ceramic particle (Bio-glass) were increased, the stress limit in the fatigue curve of nanocomposite appeared,

and the hardness values increased by (144%) at a weight fraction of 4% of Bio-glass ceramic nano-powder when compared with the pure specimen [16].

Gamal et al. examined the antibacterial effect of polymethylmethacrylate (PMMA) by mixing different concentrations (0, 0.05, 0.1, 0.15, and 1%) of nano-graphene oxide (GO) in order to overcome the PMMA drawbacks. The excessive thermal expansion and the inherent surface properties enhanced the microbial growth that led to stomatitis. The results of the research showed the improved antibacterial activity of prepared PMMA nanocomposites with 0.05% GO incorporation by exhibiting an inhibition zone that can inhibit the *Streptococcus mutans* growth, and these could be attributed to the capacity of GO in this concentration to release from the polymer matrix and spread into the agar [17].

Notwithstanding that, the previous experimental studies have highlighted the promising properties of polymethyl methacrylate that are reinforced by nano material and used in many applications. However, there is none of these previous experimental studies used the ultrasonic mixing method to dispersion nanoparticles into PMMA matrix, and in addition the application of these samples as cartilaginous joints. This study aims to enhance the physical, biological, and mechanical characteristics of PMMA acrylic resin used in manufacturing cartilaginous joints by adding nanoparticle materials that disperse into the matrix using the ultrasonic mixing method. These composite materials comprise PMMA acrylic resin as the matrix material and the nanoparticles as reinforcement ( $\text{TiO}_2$ ,  $\text{SiO}_2$ , and Talc) powders. In addition, nano titanium oxide, silicon oxide, and Talc were selected for their excellent antibacterial with outstanding mechanical properties.

## 2. Experimental Method

### 2.1 Materials

The matrix material which is utilized in this study is acrylic resin-soft polymethylmethacrylate (PMMA) with a density of  $1.18 \text{ g/cm}^3$ , as a pour-type resin matrix material manufactured by (OrtoteK) company from Ankara in Turkey. The reinforcement materials were used in different percentage ratios of ceramic nanoparticles, including  $\text{TiO}_2$ ,  $\text{SiO}_2$ , and Talc from (Skyspring Nanomaterials, Inc. USA) with a purity of 99.5%.

### 2.2 Preparation of Nanocomposite Material

The number of reinforced materials ( $\text{TiO}_2$ ,  $\text{SiO}_2$ , and Talc) necessary for filling the mold cavities was measured using an electronic balance based on the overall weight of the matrix material PMMA required by utilizing the theory of mixing rule. Utilizing the ultrasonic mixing technique, the liquid monomer (MMA) and one kind of nanoparticles ( $\text{TiO}_2$ ,  $\text{SiO}_2$ , and Talc) should be homogeneously and continuously mixed at room temperature for (20-30 min). Therefore, it must be confident that it is homogeneous before adding PMMA powder (hardener) to the mixture to create composite materials. The powder was then gradually added to the mixture and stirred in. At last, nanocomposite materials were prepared, injected into the silicon mold, and kept at room temperature for approximately 24 hours, according to the provided organization's guidelines. The samples were released from the silicon structure when the polymerization relieving process was completed, having a quite smooth surface. They were then exposed to room temperature in preparation for the subsequent testing.

## 3. Characterization

### 3.1 Particles Size Analyzer

Based on the principles of Dynamic Light Scattering (DLS) of a model Brookhaven instrument from Holtsville, in New York, United States, and after the ultrasonic dispersion in water for 10 min, the sample was put into the device utilizing the 90Plus to analyze the samples from less than 1 nm to 6  $\mu\text{m}$  for estimating the size and distribution of particles. This analysis was done in the Advanced Materials Research Center at the University of Technology.

### 3.2 The Fourier Transform Infrared (FT-IR) Spectra Test

The FT-IR technique was used to get detailed information on the molecular structure and chemical bonds of polymer materials. This was conducted according to the standards ASTM E1252 using a Fourier Infrared (FI) spectrometer made by the Bruker Optics company type (TENSOR-27). In the (400-4000)  $\text{cm}^{-1}$  range, the infrared spectrum was used.

### 3.3 Tensile Test

The specimens were tensile tested in accordance with ASTM D 638. This test was performed using a universal tensile instrument manufactured by (Laryee Company in China), type (WDW-50) at a cross-head speed of 5 mm/min. The tensile load was applied at the ambient temperature until the specimens failed, and a stress-strain curve was obtained [18].

### 3.4 Compression Test

According to ASTM D-695, the specimen's compression test was accomplished using a universal test machine, and the compression load was introduced and raised steadily till the specimen was destroyed. This test was carried out with an identical device used for tensile tests at a cross-head speed of 5 mm/min [19].

### 3.5 Hardness Test

Hardness is a solid material property described as the material's surface resistance to penetration, abrasion, wear, and scratching. The volume percentage of reinforced particles, temperature, intermolecular bonds, chain structure, and particle size influence the hardness test. Shore A test was used to determine the hardness of the samples that have a smooth, plain surface with a thickness of at least 3 mm and are not subjected to mechanical vibrations, such that the prepared specimen has a diameter of 30 mm and a thickness of 4 mm [14,20].

### 3.6 Surface Roughness Test

The Surface Roughness Tester (TR200) device is a good tool for estimating the surface roughness value using identical specimens as in the hardness test. It is equipped with a moving sensor that travels linearly over the test material's surface, the sensor was moved in accordance with the profile of the surface. This movement was translated into an electrical signal amplified and transferred into digital signals. To acquire more detailed findings, each specimen was tested three times in different locations, and the average results were obtained. This test aims to evaluate the influence of the reinforcing material on the micrometry of the tested surface specimens [21].

### 3.7 Density Test

The specimens were prepared according to the ASTM standard for density testing (D-792). The density of the specimens was determined using Archimedes' method and a precise balance of the following type: PS3/C/1 device. Any size of the specimen can be used in this test, but the volume can be at least 1 cm<sup>3</sup>, with clean and smooth surface specimens. The test specimens must be weighed in the air and distilled water. By taking the specific gravity and multiplying it by the deionized water density, the specific gravity is then converted into density [22]:

$$\text{Specific Gravity (Sp. Gr)} = \frac{M_d}{(M_d + M - M_i)} \quad (1)$$

$$\text{Density} = (\text{Sp. Gr}) * (0.997) \quad (2)$$

where:  $M_d$ : The sample mass in the air (gm).  $M_i$ : The sample mass in water (gm).  $M$ : Mass of the partially immersed wire (about 0.02 gm)

### 3.8 Water Absorption Test

This test was achieved in accordance with the standard ASTM D570. This test requires measuring the weight of the samples and after that immersing the patterns entirely in a water container at the ambient conditions for approximately one day. The specimens were extracted from the water container, dried with a clean cloth, and weighed using an electronic balance. The water absorption was obtained by using Equation 3 [22]:

$$\text{Percentage of Water Absorption} = \frac{W_s - W_d}{W_d} * 100 \quad (3)$$

where:  $W_d$ : The sample mass before immersion in distilled water.  $W_s$ : The sample mass after immersion for one day in distilled water.

### 3.9 Antibacterial Effect Test

This test was performed to evaluate the antibacterial (biological) activity of the prepared samples against two types of bacteria, which are *Streptococcus mutans* (*S. mutans*) and *Staphylococcus aureus* (*S. aureus*). After being incubated at 37°C for 24 hours, many microlitres (106 bacteria) of bacteria solution were evenly spread over Mueller-Hinton agar, and the diameters of (6 mm) of the PMMA composite discs were placed on the agar. The antibacterial effectiveness of the cement samples was then measured by measuring the inhibitory zone that developed around them.

## 4. Results and Discussion

### 4.1 Particle Size Analysis Results

Figure 1 (A, B, C) shows the particle size distribution of materials ( $\text{TiO}_2$ ,  $\text{SiO}_2$ , and Talc) powders, respectively. Figure 1(A) exhibits the particle size of the  $\text{TiO}_2$  with a mean diameter of about (57.3 nm). Figure 1(B) presents the particle size of the  $\text{SiO}_2$  with a mean diameter (67.8 nm), and Figure 1(C) depicts the particle size of talc powder with a mean diameter of (87.7 nm).

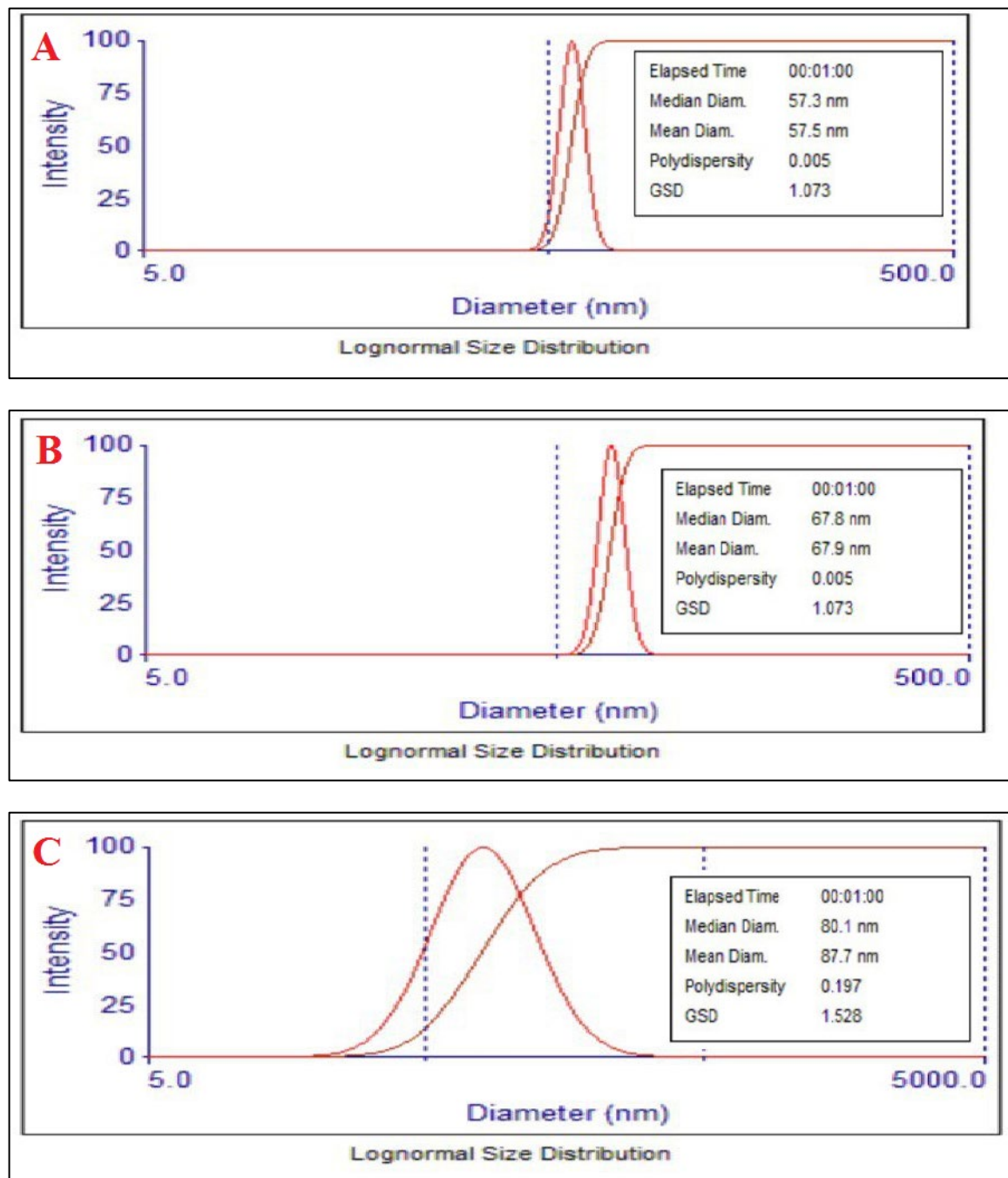
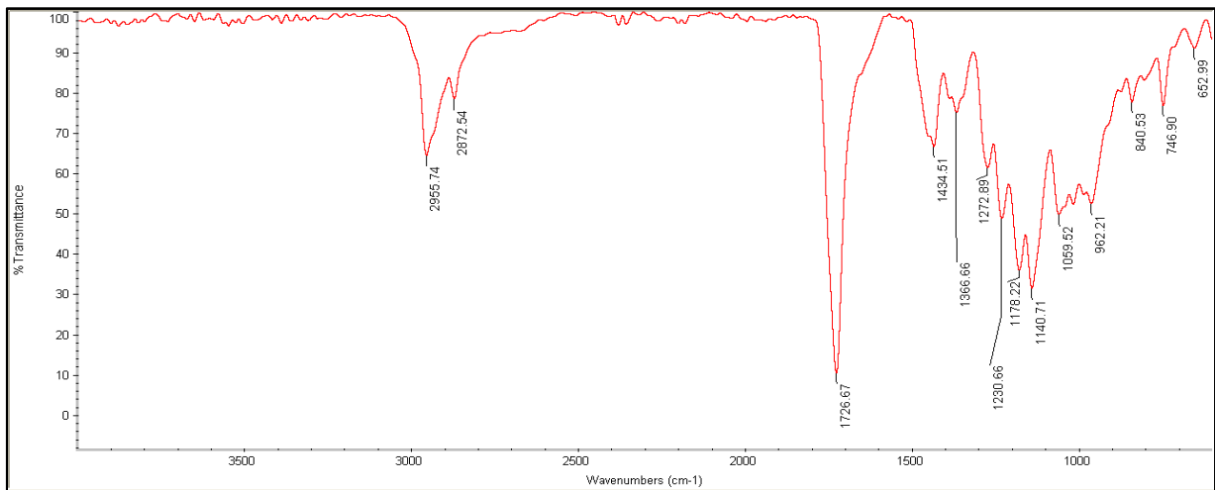


Figure 1: The Particle Size Distribution of (A) TiO<sub>2</sub>, (B) SiO<sub>2</sub>, and (C) Talc powder

#### 4.2 FT-IR Spectrometers Test Results

The characteristic functional groups associated with Nano-ceramic particles and PMMA in the composites were confirmed by FT-IR spectroscopy. The infrared spectrum of pure PMMA is shown in Figure 2, with transmittances at (2956.74 and 2872.54  $\text{cm}^{-1}$ ) with a medium look that is associated with the stretched (C-H) bond in the  $-\text{CH}_2$  and  $-\text{CH}_3$  groups, respectively. The pure PMMA sample has a peak at (1726.67  $\text{cm}^{-1}$ ) which is associated with the C=O stretching band. The characteristic band that appeared at (1434.51 and 1366.66  $\text{cm}^{-1}$ ) is related to the methyl group (C-H) bending. The peak at (1272.89-1230.66  $\text{cm}^{-1}$ ) is associated with C-O bond stretching in the ester group. The two bands at (1140.71 and 1059.52  $\text{cm}^{-1}$ ) are caused by  $\text{CH}_3$  twisting, while the band at (1178.22  $\text{cm}^{-1}$ ) corresponds to  $\text{CH}_3$  wagging. The C-C stretching-induced vibration modes are seen at (962.21  $\text{cm}^{-1}$ ). The (840.53  $\text{cm}^{-1}$ ) peak is attributed to  $\text{CH}_2$  rocking, and the reason for the peak at (746.90  $\text{cm}^{-1}$ ) is the  $\text{CH}_2$  bending and rocking in and out of a plane.



**Figure 2:** FT-IR spectrum of the pure PMMA material

To fully characterize the PMMA composite samples band both before and after the inclusion of ceramic nanoparticles at different weight fractions, the infrared spectra of PMMA composites reinforced with (0.5, 1, and 1.5%) weight fraction of ceramic nanoparticles ( $\text{SiO}_2$ ), ( $\text{TiO}_2$ ) and (Talc) are revealed in Figures 3, 4 and 5, respectively. The infrared spectra of PMMA composite specimens showed the characteristic vibration bands of neat PMMA, as displayed in Figure 2. Additionally, no new peaks were identified for the PMMA composite samples with the presence of ceramic nanoparticles, as confirmed by the infrared spectra. This is owing to the lack of cross-linking in these specimens, as well as the finding of a physical bond.

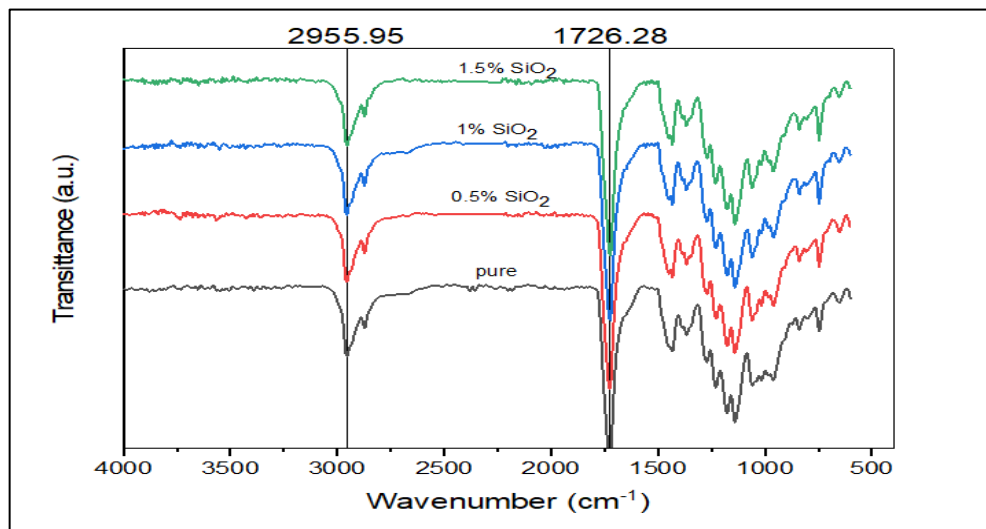


**Figure 3:** FT-IR spectrum of the PMMA composite containing nano  $\text{SiO}_2$  particles at various content ratios

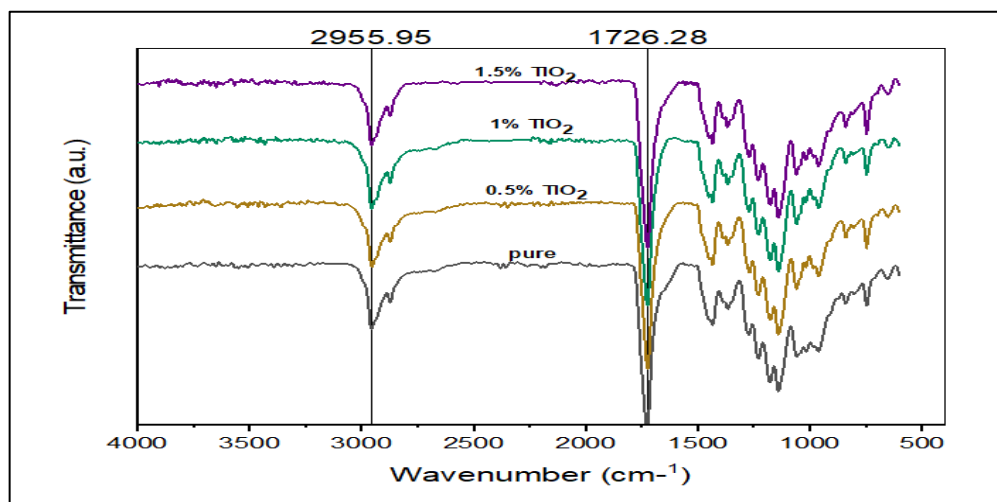


**Figure 4:** FT-IR spectrum of the PMMA composite containing nano  $\text{TiO}_2$  particles at various content ratios

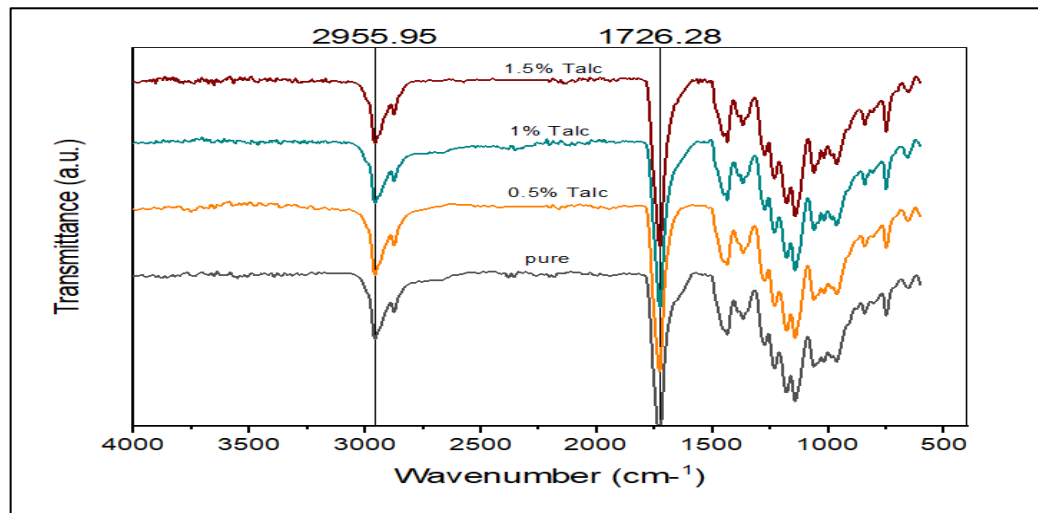


Figure 5: FT-IR spectrum of the PMMA composite containing nano Talc particles at various content ratios

### 4.3 Tensile Strength Results

The tensile strength of the PMMA composite samples reinforced with ( $\text{TiO}_2$ ,  $\text{SiO}_2$ , and Talc) nanoparticles are shown in Figure 6. From the figure, the results of tensile strength illustrated that the addition (0.5, 1, and 1.5%) of  $\text{SiO}_2$  improved the tensile strength by (16.6, 51.2 and 66.5%), while the inclusion (0.5, 1, and 1.5%) of  $\text{TiO}_2$  enhanced the tensile strength by (25, 44.9 and 47.55%), and the addition of (0.5, 1 and 1.5%) of Talc improved the tensile strength of PMMA by (30.2, 50 and 59.3%). So, from this figure, it can be concluded that the polymer composite (PMMA) reinforced with 1.5% nanoparticles has the highest tensile strength. The improvement of tensile strength is due to the strengthening mechanism which mentioned the amount of these particles that played an important role by obstructing the motion of PMMA chains. And, the good wettability of these particles by (MMA) liquid may cause an increase in the bonding force between the matrix and reinforced material, so the resultant composites will require high stress to break their physical bonding [23].

Figure 7 evinces that the elastic modulus of the PMMA polymer composite samples strengthened with (0.5, 1, and 1.5%)  $\text{SiO}_2$  improved at a rate of (100, 220.7, and 261.5%). In contrast, the addition of  $\text{TiO}_2$  at (0.5, 1, and 1.5%) enhanced the elastic modulus at the rate (153, 273, and 315.38%) and the modulus of elasticity of PMMA enhanced by (261.5, 307.69, and 338.4%) via adding (0.5, 1 and 1.5%) Talc. For each type of three different types of nanopowders utilized, the elastic modulus increases as the weight fraction rises. This is related to the nature of the bonding and strengthening. Additionally, the higher stiffness of these nanoparticles than the PMMA matrix owing to their higher elastic modulus of powder results in an improvement in the stiffness of composite samples. There is also the possibility of matrix-particle interaction with the increased nanoparticle concentration, which causes an increase in the stress activity traveling from the matrix phase to the particle phase, as mentioned in [24].

This behavior might be attributed to the nanoparticles' widespread and uniform distribution, which reduces the agglomeration (grouping) of reinforcement materials. As well as, the high interfacial bonding between the nano reinforcements and the PMMA matrix was established, and the slippage of the PMMA chains was decreased by occupying the spaces inside the PMMA matrix, producing a positively enhanced modulus of elasticity and ultimate tensile strength [25].

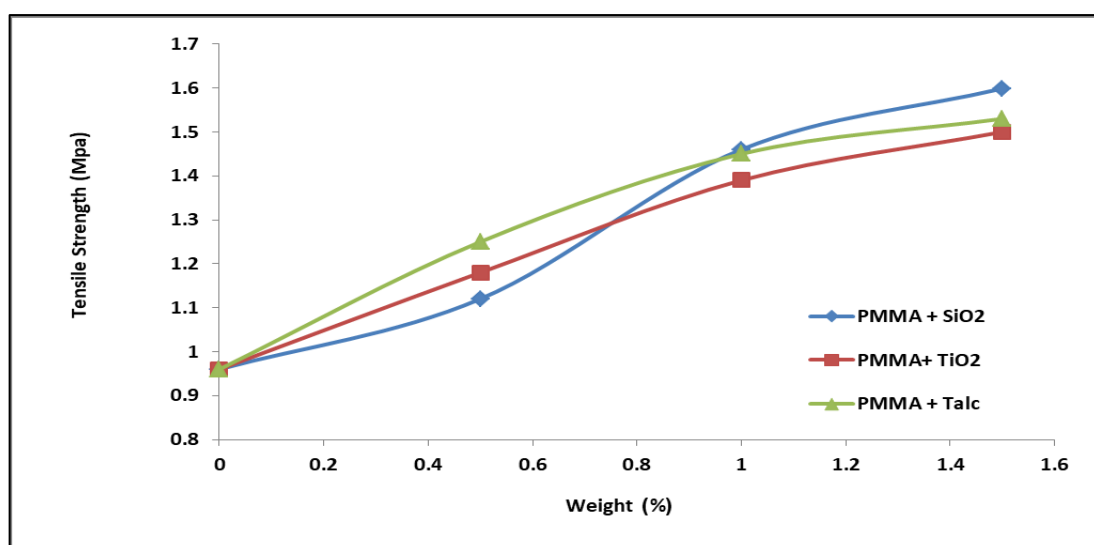
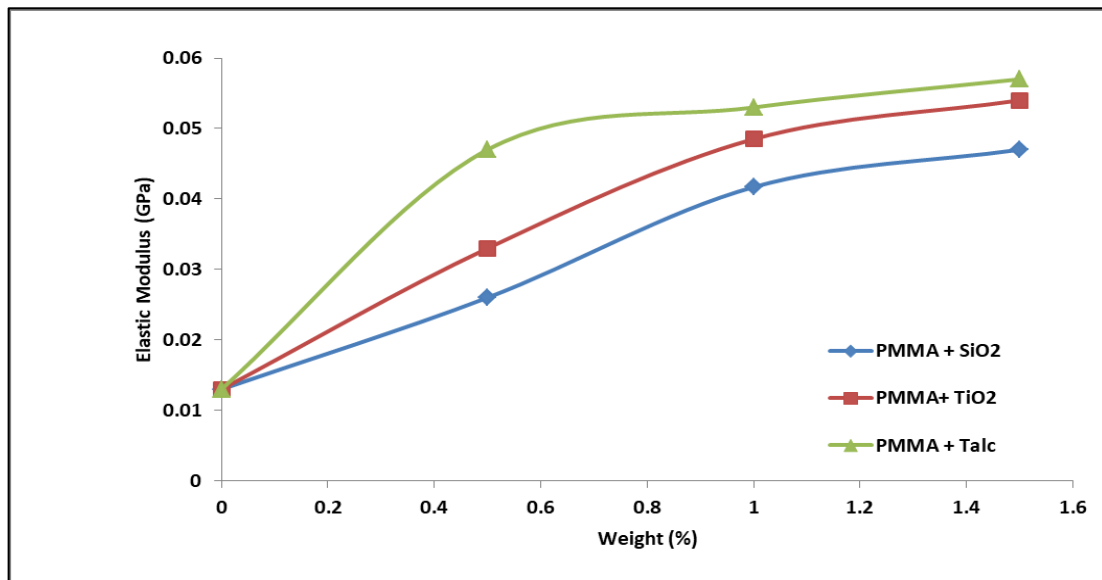
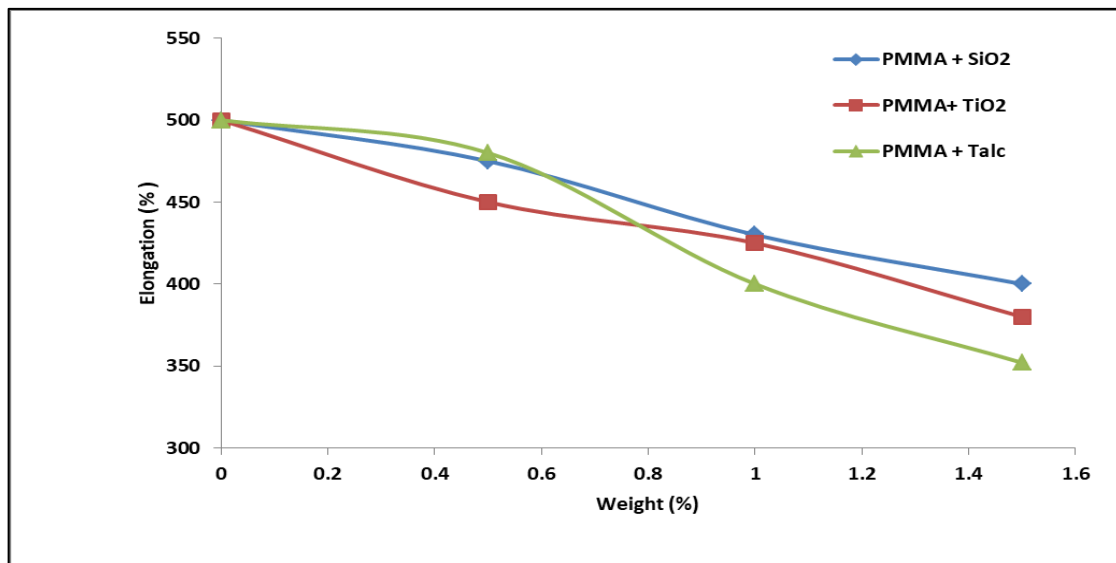


Figure 6: Tensile Strength of the composite PMMA polymer strengthened with ceramic nanoparticles



**Figure 7:** Elastic Modulus of the composite PMMA polymer strengthened with ceramic nanoparticles

As shown in Figure 8, the elongation percentage was slightly reduced by the inclusion of nanoparticles; owing to the fact that the elongation (tensile strain) is dependent on the interfaces bonding between the matrix material and the supporting substances (nano-SiO<sub>2</sub>, nano-TiO<sub>2</sub>, and nano-Talc) particles. Because of the reinforcing behavior of these nanoparticles, it limits the polymer chain's slippage, as well as the consequence PMMA matrix and inclusion material with more excellent adhesive and compatibility [26, 27].



**Figure 8:** Elongation Percentage of the composite PMMA polymer strengthened with ceramic nanoparticles

#### 4.4 Compressive Strength Results

The compression strength for the PMMA composite samples reinforced with (TiO<sub>2</sub>, SiO<sub>2</sub>, and Talc) nanoparticles are manifested in Figure 9. This figure shows that the addition (0.5, 1, 1.5%) of SiO<sub>2</sub> improved the PMMA compressive strength by (10.5, 32, and 49.3%), while the inclusion (0.5, 1, 1.5%) of TiO<sub>2</sub> enhanced the compressive strength of PMMA by (3.4, 16.6, 36.66%), and the addition of (0.5, 1, 1.5%) of Talc improved the compression strength of PMMA by (4, 21.3, 40.5%). So, it can be concluded that the compression strength of composite specimens increases as the weight fraction of nanoparticles raises. It is believed that the enhanced strength during the compression is due to the strong interaction and reasonable adhesion force among the elements of the reinforcement materials (ceramic nanoparticles) of the PMMA matrix, which result in the stiffening of polymer chains by inhibiting the movement of crack and molecular motion of the prepared bio-composite samples, thereby showing a good resistance under vertical load applied [27].

The highest compressive strength is obtained from 1.5 weight percent (SiO<sub>2</sub>) due to the ability of silicon oxide nanoparticles to obstruct the propagation of cracks inside the PMMA matrix based on the enhancing mechanism and the good bond strength between the matrix and these nanopowders, as previously indicated [23].



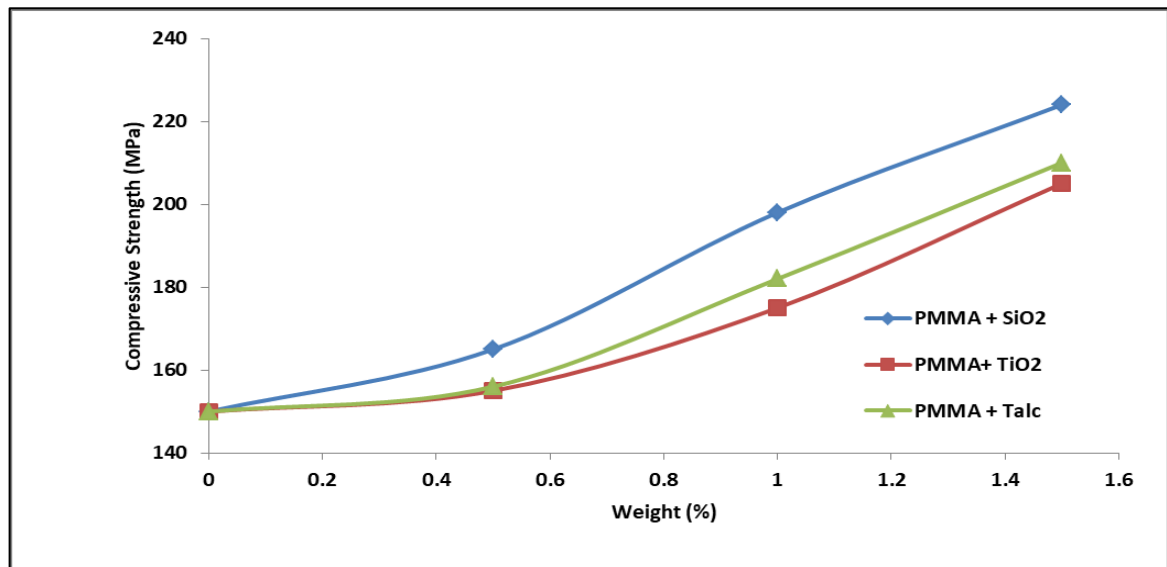


Figure 9: Compressive Strength of the composite PMMA polymer strengthened with ceramic nanoparticles

#### 4.5 Hardness Results

Figure 10 illustrates the relationship between the hardness of PMMA samples and the concentration of ceramic nano-powders (TiO<sub>2</sub>, SiO<sub>2</sub>, and Talc). This figure demonstrates that the addition (0.5, 1, 1.5%) of SiO<sub>2</sub> nanoparticles to PMMA improved the hardness by (15.2, 31.25, and 41.66%), while the inclusion (0.5, 1, 1.5%) of TiO<sub>2</sub> with PMMA increased the hardness by (6.8, 14.59, 20.83%), and the addition of (0.5, 1, 1.5%) of Talc enhanced the hardness of PMMA by (10.41, 22.91, 31.6.3%). Furthermore, the increased weight percentage of adding ceramic nano-powders raises the hardness values of samples. This is attributed to the substantial compatibility of the polymeric matrix (PMMA) elements with the inclusion of nano-powders (TiO<sub>2</sub>, SiO<sub>2</sub>, and Talc). Also, the ceramic particle's hardness may be more substantial and stiffer than the PMMA polymer matrix control sample. Moreover, the formation of strong cross-links linking or supramolecular bonding between the powders and the matrix that cover or shield the nano additives allows the interface between them to transfer the force and therefore increase the hardness. So, the addition of (SiO<sub>2</sub>, TiO<sub>2</sub>, and Talc) nanoparticles results in a tougher (harder) surface and an excellent barrier to matrix mobility under the force direction, as stated in [28].

The explanation for this behavior is that the addition of (SiO<sub>2</sub>, TiO<sub>2</sub>, and Talc) particles improves the material's mechanical properties while also having a high degree of compatibility among the ingredients in composite materials.

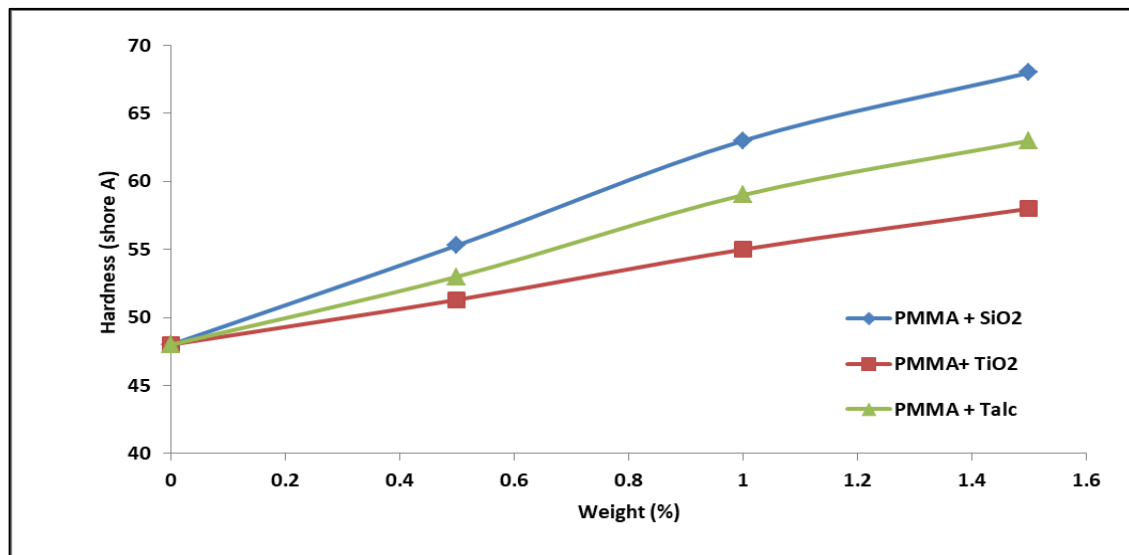


Figure 10: Hardness (Shore A) of the composite PMMA polymer strengthened with ceramic nanoparticles

#### 4.6 Surface Roughness Results

Figure 11 elucidates the surface roughness and the weight fraction of nanocomposite samples relationship based on the PMMA matrix and strengthened by ceramic nano-powders (TiO<sub>2</sub>, SiO<sub>2</sub>, and Talc). This figure reflects that when the weight percentage of reinforcement in the polymer matrix used to form the bio-composite material samples is increased, the value of surface roughness for the samples diminished. The surface roughness results showed that the addition (0.5, 1, 1.5%) of SiO<sub>2</sub>,

TiO<sub>2</sub> and Talc particles reduced the surface roughness by (14.28, 39.22 and 48.57%), (9.42, 31.14, and 51.14%), and (11.65, 28.88 and 42.47%), respectively. These results were associated with the properties, the surface wettability degree of the reinforcing materials (TiO<sub>2</sub>, SiO<sub>2</sub>, and Talc) nano-particles distributed throughout the polymer matrix, and the size of tiny particles (nano-particles) utilized, as mentioned [21, 27].

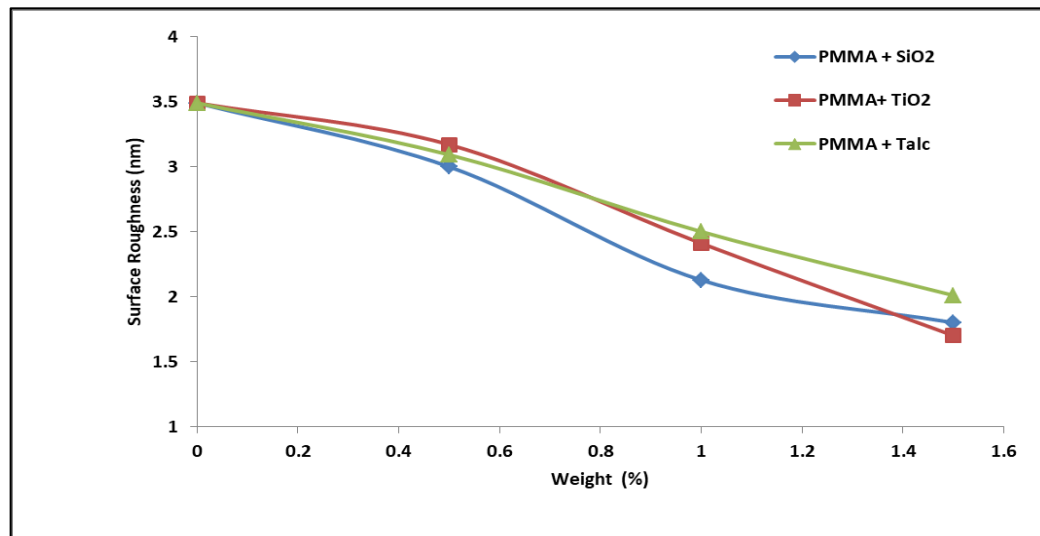


Figure 11: Surface Roughness of the composite PMMA polymer strengthened with ceramic nanoparticles

#### 4.7 Density

The density results of composite specimens and the percentage of nanoparticles included in the PMMA matrix (TiO<sub>2</sub>, SiO<sub>2</sub>, and Talc) are portrayed in Figure 12. The density results showed that the PMMA reinforced with (0.5, 1, 1.5%) SiO<sub>2</sub> decreased the density by (3.8, 7.61, and 10.45%). In contrast, the inclusion of (0.5, 1, and 1.5 %) TiO<sub>2</sub> reduced the density by (5.71, 9.5, 11.7%), and the addition of (0.5, 1, 1.5%) of Talc decreased the density of PMMA nanocomposite by (2.95, 5.81, 9.63%). When the number of nanoparticles in the polymer composite was increased, it was discovered that the density slightly dropped when compared to the matrix material. These components are very compatible [28, 29].

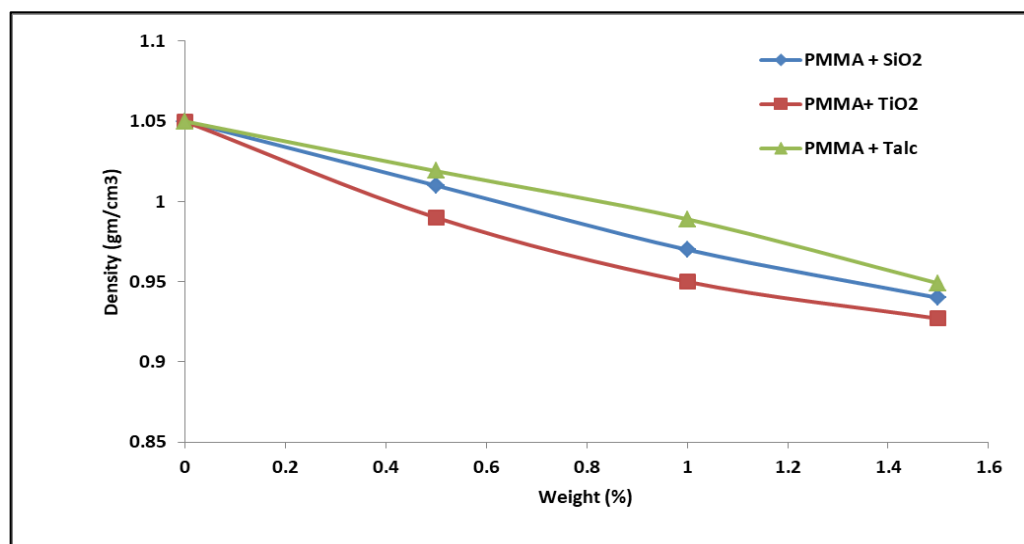


Figure 12: Density of the composite PMMA polymer strengthened with ceramic nanoparticles

#### 4.8 Water Absorption

Figure 13 depicts the water absorption association with the nanoparticle concentration ratios in composites. From this figure, it can be concluded that including the SiO<sub>2</sub> into the PMMA matrix at (0.5, 1, and 1.5%) increased the water absorption by (14.28, 76.2, and 188.5%). In contrast, the addition of TiO<sub>2</sub> at (0.5, 1, 1.5%) enhanced the water absorption by (22.85, 80, and 152.2%), and the addition of (0.5, 1, 1.5%) of Talc improved the water absorption of PMMA by (22.8, 49.14 and 125.71%). The water absorption property was discovered to rise with increasing the nanoparticle percentage in the polymer matrix composites; this may be attributed to the matrix material's inability to effectively saturate the additives at a more significant portion, which most probably assisted the moisture entry [29,30].

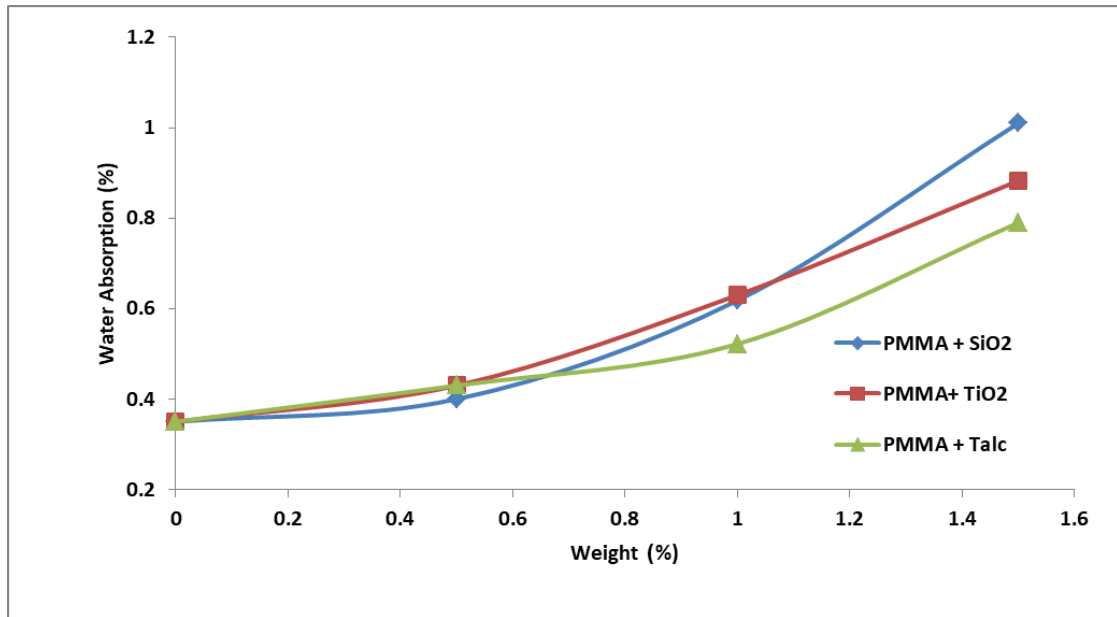


Figure 13: Water Absorption of the composite PMMA polymer strengthened with ceramic nanoparticles

### 4.9 Antibacterial Effect Results

The results of antibacterial tests using two types of bacteria *Streptococcus mutans* (*S. mutans*) and *Staphylococcus aureus* (*S. aureus*) on the PMMA pure and PMMA composite samples reinforced with ( $\text{SiO}_2$ ,  $\text{TiO}_2$ , and Talc) nanoparticles are viewed in Figures 14 (A,B,C), 15 (A,B,C) and 16 (A,B,C), respectively. From these results, the  $\text{TiO}_2$ ,  $\text{SiO}_2$ , and Talc nanocomposite samples exhibited good antibacterial effects against *Streptococcus mutans* (*S. mutans*) and *Staphylococcus aureus* (*S. aureus*), respectively. When the particles are added to the polymer matrix, the antibacterial properties enhance with the increased loading of particles in the composite samples due to the influence of these nanoparticles' antibacterial activity, so all the groups exhibited strong antibacterial effects against the two types of bacteria. Regarding the composite samples, it was found that the highest amount of nanoparticles in the matrix material produced the most outstanding results. In addition, the inhibition zone grew more significantly as the reinforcement concentration was increased, and the bacterial growth was restricted.

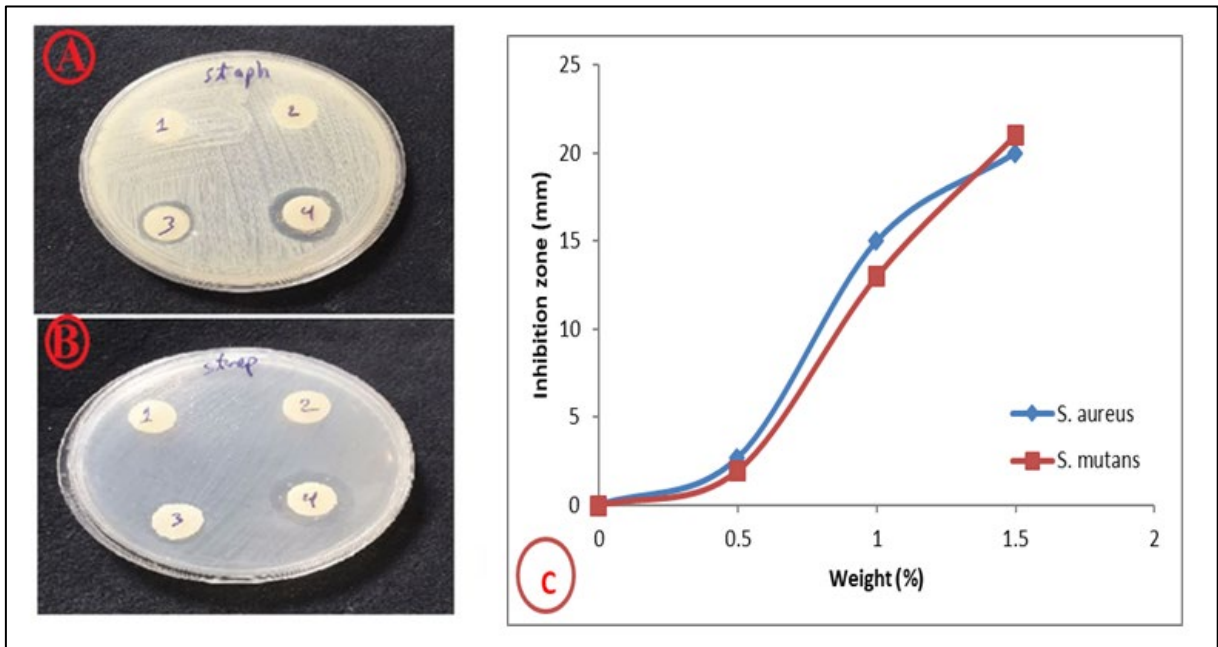
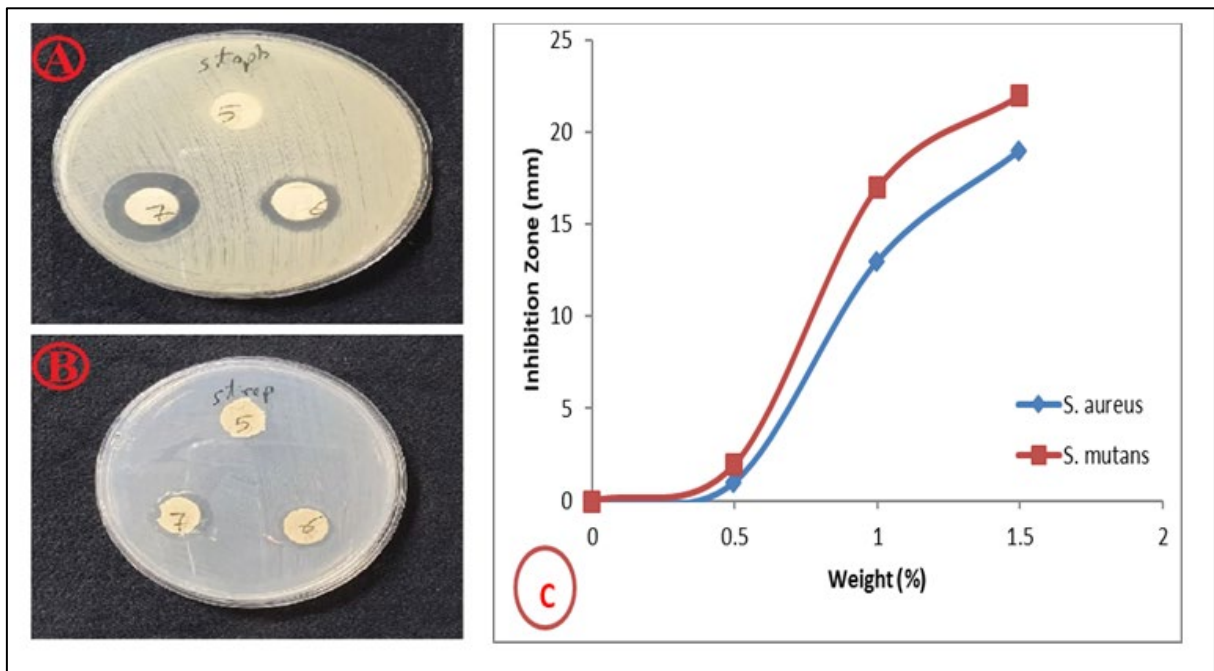
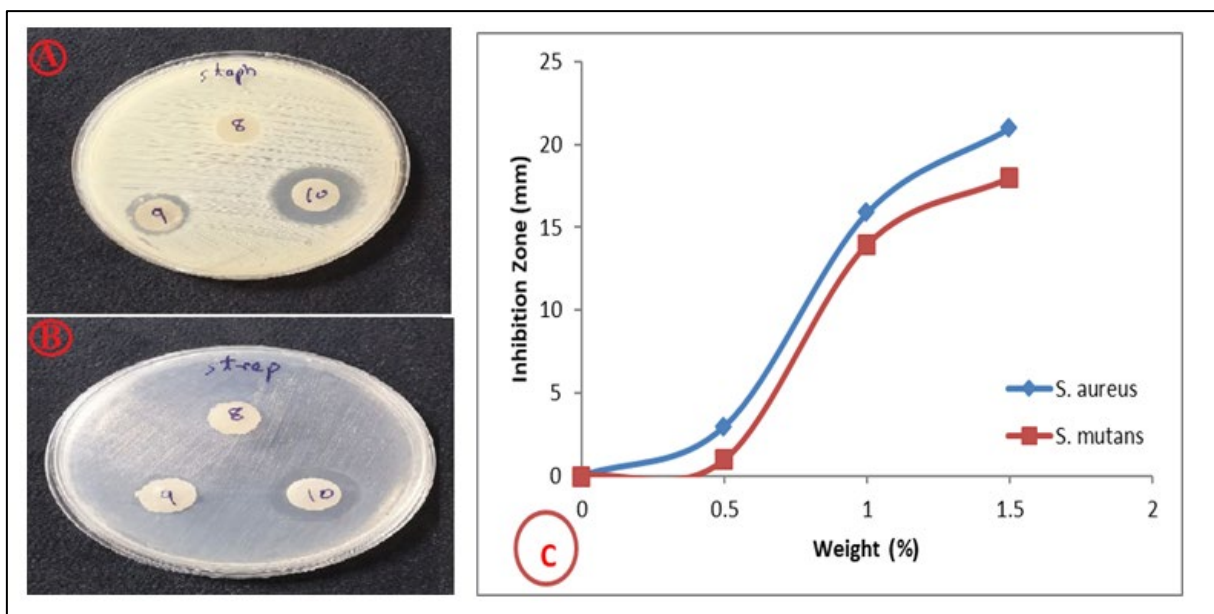


Figure 14: (A, B) Images of the pure and composite samples containing nano  $\text{SiO}_2$  particles after 24 hr for *S. aureus* and *S. mutans* respectively, (C) The inhibition Zone Size with *S. mutans* and *S. aureus*



**Figure 15:** (A, B) Images of the composite samples containing nano TiO<sub>2</sub> particles after 24 hr for *S. aureus* and *S. Mutans*, respectively, and (C) The inhibition zone size with *S. mutans* and *S. aureus*



**Figure 16:** (A, B) Images of the composite samples containing nano Talc particles after 24 hr for *S. aureus* and *S. Mutans*, respectively, and (C) The inhibition zone size with *S. mutans* and *S. aureus*

## 5. Conclusion

From the experimental results of the polymer nanocomposites manufacture by the addition of TiO<sub>2</sub>, SiO<sub>2</sub>, and Talc nanoparticles, the following can be concluded:

- 1) The tensile properties of the polymer nanocomposite improved with the increasing inclusion of nano-powders (TiO<sub>2</sub>, SiO<sub>2</sub>, and Talc) in the polymer matrix PMMA, despite of the reduction of elongation at break. The highest rate of increase in the tensile strength of nanocomposites was (66.5%) obtained for silicon oxide samples at (1.5 wt.%), and the best improvement in the elastic modulus of samples was obtained by adding 1.5% SiO<sub>2</sub>.
- 2) The compressive strength of the pure PMMA samples is poorer than that of samples strengthened with TiO<sub>2</sub>, SiO<sub>2</sub>, and Talc nano-powders. The maximum rate of improvement in the compressive strength of nanocomposites was (49.3%) for the silicon oxide samples at (1.5 wt.%).

- 3) Compared to pure PMMA, the polymer composite's hardness (Shore A) was enhanced by raising the powder filler loading (TiO<sub>2</sub>, SiO<sub>2</sub>, and Talc), and the best rate of hardness increase was (41.66%) for the nanocomposite samples reinforced with the SiO<sub>2</sub> nanoparticles.
- 4) The density property decreases after adding TiO<sub>2</sub>, SiO<sub>2</sub>, and Talc to the PMMA matrix, while including the nano-powders leads to raised water absorption results.
- 5) The addition of 1.5% of each type of ceramic nanoparticles (TiO<sub>2</sub>, SiO<sub>2</sub>, and Talc) to the PMMA matrix results in the most excellent antibacterial effects against *Streptococcus mutans* (*S. mutans*) and *Staphylococcus aureus* (*S. aureus*) bacterial.
- 6) This study focuses on the requirement for novel, inexpensive, environmentally acceptable materials for medicine and the creation of materials utilized for cartilaginous joints.

### Author contributions

Conceptualization, A. Shafer, A. Al.Zubaidi, W. Salih; methodology, A. Al.Zubaidi; validation, W. Salih; resources, A. Shafer; data curation, W. Salih; writing—original draft preparation, W. Salih; writing—review and editing, W. Salih; supervision, A. Al.Zubaidi. All authors have read and agreed to the published version of the manuscript.

### Funding

This research received no specific grant from any funding agency in the public, commercial, or not-for-profit sectors.

### Data availability statement

The data that support the findings of this study are available on request from the corresponding author.

### Conflicts of interest

The authors declare that there is no conflict of interest.

### References

- [1] J. K. Oleiwi, A. Hamad, H. Jabbar, and A. Rahman, Experimental Investigation of Flexural and Impact Properties of PMMA Reinforced by Bamboo and Rice Husk Powders, *Int. J. Mech. Eng. Technol.*, 9 (2018) 559–568.
- [2] Sa, Y., Yang, F., Wang, Y., Wolke, J.G.C., Jansen, J.A. 2018. Modifications of Poly(Methyl Methacrylate) Cement for Application in Orthopedic Surgery, *Advances in Experimental Medicine and Biology*, vol 1078, pp 119–134. Springer, Singapore. [https://doi.org/10.1007/978-981-13-0950-2\\_7](https://doi.org/10.1007/978-981-13-0950-2_7)
- [3] S. S. Eil Bakhtiari, S. Karbasi, S. A. Hassanzadeh Tabrizi, R. Ebrahimi-Kahrizsangi, and H. Salehi, Evaluation of the effects of chitosan/multiwalled carbon nanotubes composite on physical, mechanical and biological properties of polymethyl methacrylate-based bone cements, *Mater. Technol.*, 35 (2020) 267–280. <https://doi.org/10.1080/10667857.2019.1678086>
- [4] R. Choudhary, S. K. Venkatraman, I. Bulygina, F. Senatov, S. Kaloshkin, and S. Swamiappan, Designing of porous PMMA/diopside bone cement for non-load bearing applications, *J. Asian Ceram. Soc.*, 8 (2020) 862–872. <https://doi.org/10.1080/21870764.2020.1793476>
- [5] S. Kadhun Alsaedi, S. Salih, and F. Hashim, Preparation and Characterization of Polymer Blend and Nano Composite Materials Based on PMMA Used for Bone Tissue Regeneration, *Eng. Technol. J.*, 38 (2020) 501-509. <https://doi.org/10.30684/etj.v38i4A.383>
- [6] S. Ahmed and W. Salih, Development the Mechanical Properties of the Acrylic Resin (PMMA) by Added Different Types of Nanoparticles, Used for Medical Applications, *Eng. Technol. J.*, 40 (2021), 166–171. <https://doi.org/10.30684/etj.v40i1.2017>
- [7] R. E. Nuñez-Anita, L. S. Acosta-Torres, J. Vilar-Pineda, J. C. Martínez-Espinosa, J. de la Fuente-Hernández, and V. M. Castaño, Toxicology of antimicrobial nanoparticles for prosthetic devices, *Int. J. Nanomed.*, 9 (2014) 3999–4006.
- [8] L. Chen et al., Silicate bioceramic/PMMA composite bone cement with distinctive physicochemical and bioactive properties, *R. Soc. Chem.*, 5 (2015) 37314-37322. <https://doi.org/10.1039/C5RA04646G>
- [9] F. Pahlevanzadeh, H. R. Bakhsheshi-Rad, A. F. Ismail, M. Aziz, and X. B. Chen, Development of PMMA-Mon-CNT bone cement with superior mechanical properties and favorable biological properties for use in bone-defect treatment, *Mater. Lett.*, 240 (2018) 9–12. <https://doi.org/10.1016/j.matlet.2018.12.049>
- [10] W. BDAIWI, Reinforcement of Poly(MethylMethaAcrylate) by ZrO<sub>2</sub>Y<sub>2</sub>O<sub>3</sub> Nanoparticles Used in Medical Applications, *J. Optoelectron. Biomed. Mater.*, 10 (2018)1-10.
- [11] B. J. Obeid, F. K. farhan, and E. J. Mohammed, Improving some mechanical properties of the system (PMMA-ZrO<sub>2</sub>) used in medical applications, *J. Adv. Res. Dyn. Control Syst.*, 10 (2018) 1954–1959.

- [12] A. Zore, A. Abram, A. U<sup>ˆ</sup>, I. Godina, F. Rojko, and R. Štukelj, Antibacterial Effect of Polymethyl Methacrylate Resin Base Containing TiO<sub>2</sub> Nanoparticles, *Coatings*, 12 (2022) 1757. <https://doi.org/10.3390/coatings12111757>
- [13] H. Asgharzadeh Shirazi, M. Ayatollahi, M. Navidbakhsh, and A. Asnafi, New insights into the role of Al<sub>2</sub>O<sub>3</sub> nano-supplements in mechanical performance of PMMA and PMMA/HA bone cements using nanoindentation and nanoscratch measurements, *Mater. Technol.*, 36 (2021) 212–220. <https://doi.org/10.1080/10667857.2020.1741939>
- [14] A. Abdullah, H. Jaber, and H. Al-Kaisy, Impact Strength, Flexural Modulus and Wear Rate of PMMA Composites Reinforced by Eggshell Powders, *Eng. Technol. J.*, 38 (2020) 960–966. <https://doi.org/10.30684/etj.v38i7a.384>
- [15] S. K. Al-Janabi, M. H. Al-Maamori, and A. J. Braihi, Experimental and Numerical Investigation of PMMA Based Composites used for Bone Cement Application, *IOP Conf. Ser. Mater. Sci. Eng.*, 1090 (2021) 012082. <https://doi.org/10.1088/1757-899x/1090/1/012082>
- [16] A. Bashir, F. K. Farhan, and H. A. Yasr, Biomechanical Properties of PMMA/Bio glass Ceramic, *Ann. Rom. Soc. Cell Biol.*, 25 (2021) 8859–8866.
- [17] R. Gamal, Y. Gomaa, and A. Said, Incorporating nano graphene oxide to poly-methyl methacrylate; antibacterial effect and thermal expansion., *J. Mod. Res.*, 1 (2019) 19–23. <https://doi.org/10.21608/jmr.2019.14281.1003>
- [18] A. B. of A. Standard, Standard Test Method for Tensile Properties of Plastics, D 638-87 b, 9 (1988) 1–17.
- [19] Annual Book of ASTM Standard, Standard Test Method for Compressive Properties of Rigid Plastics, 2002.
- [20] ASTM D2240-00, Standard method for Rubber Property - Durometer Hardness, Annual Book of ASTM Standarts, 2017.
- [21] H. Sadeq, S. Salih, and A. Braihi, Development of Surface Roughness and Mechanical Properties of PMMA Nanocomposites by Blending with Polymeric Materials, *Eng. Technol. J.*, 37 (2019) 558–565. <https://doi.org/10.30684/etj.37.12a.10>
- [22] S. H. Ahmed and W. M. Salih, Enhancement of the Characteristics for Polymeric Blend (PMMA/UP) Used in Socket Prosthetic, *AIP Conf. Proc.*, 2437, 2022, 020001. <https://doi.org/10.1063/5.0096384>
- [23] D. Q. Adnan Hamad, Study of Flexural and Impact Properties of Nanohybrid Composites Materials By Using Poly Methyl Methacrylate (Pmma) Matrix, *J. Eng. Sustain. Dev.*, 23 (2019) 114–127. <https://doi.org/10.31272/jeasd.23.3.9>
- [24] A. Basim Abdul-Hussein, F. Abbas Hashim, and T. Raad Kadhim, Effect of Nano Powder on Mechanical and Physical Properties of Glass Fiber Reinforced Epoxy Composite, *Al-Khwarizmi Eng. J.*, 12 (2016) 72–79.
- [25] B. Email, Study the Effect of Fibers Volume Fraction and their Orientations on the Properties of the Hybrid Composite Materials, *Eng. Technol. J.*, 31A (2013) 2433–2447.
- [26] X. D. Yu, M. Malinconico, and E. Martuscelli, Highly Filled Particulate Composite Enhancement Of Performances By Using Compound Coupling Agents, *J. Mater. Sci.*, 25 (1990) 3255–3261. <https://doi.org/10.1007/BF00587683>
- [27] S. H. Ahmed and W. M. Salih, Mechanical Properties of Acrylic Laminations Resin (PMMA) Reinforced by Natural Nanoparticles and Hemp Fibers, *IOP Conf. Ser. Mater. Sci. Eng.*, 1094 (2021) 012136. <https://doi.org/10.1088/1757-899x/1094/1/012136>
- [28] R. S. Raja, K. Manisekar, and V. Manikandan, Effect of fly ash filler size on mechanical properties of polymer matrix composites, *Int. J. Mining, Metall. Mech. Eng.*, 1 (2013) 34–38.
- [29] L. Costa de Medeiros Dantas, J. Paulo da Silva-Neto, T. Souza Dantas, L. Zago Naves, F. Domingues das Neves, and A. Soares da Mota, Bacterial adhesion and surface roughness for different clinical techniques for acrylic polymethyl methacrylate, *Int. J. Dent.*, 2016 (2016) 1–6. <https://doi.org/10.1155/2016/8685796>
- [30] S. Salih, J. Oleiwi, and H. Ali, Development the Physical Properties of Polymeric Blend (SR/ PMMA) by Adding various Types of Nanoparticles, Used for Maxillofacial Prosthesis Applications, *Eng. Technol. J.*, 37 (2019) 120–127. <https://doi.org/10.30684/etj.37.4a.2>